Chapter-6

6 Therapeutic Potential of Chlorophyll Functionalized Carbon Quantum Dots against Cervical Cancer

6.1 Introduction

6.1.1 Threat about Cervical Cancer

Now a days the cervical cancer is the leading cancer among females and its occurrence is more prevalent in low and middle income nations[233]. The incidence of cervical cancer is a significant worldwide health issue associated with a high rate of morbidity and mortality. According to the WHO, Cervical cancer is the fourth most frequent type of cancer among women. Worldwide, over 570000 women were diagnosed with cervical cancer in 2018 and approximately 311000 died from the disease[234]. There are various factors which are engaged in the pathogenesis of cervical cancer and among them viral factors are the leading one[235]. Diagnosis and screening of cervical cancer in early stage allows it to be a preventable and treatable disease and can reduce its occurrence[236]. Various standard therapies are being utilized as a potential treatment for cervical cancer, however these therapies generate severe ill effects that reduces its efficacy [237]. Thus, conventional approaches necessitate the incorporation of controlled release technologies and targeted drug administration in order to be more successful and less hazardous. Recently, Quantum dots have emerged as a key players to combat cancer and among them carbon quantum dots (CQDs) have gained significant advantages due to their unique qualities such as high

hydrophilicity and photo-stability, low toxicity, and long-wavelength emission which make them a biocompatible candidate [238].

6.1.2 Properties and Biological Applications of Chl-CQDs

Over the past few years, natural products are becoming the valuable sources to prepare CQDs, because of their herbal and non-toxic attribute. The cytotoxicity is dependent on the kind and charge of the functional groups. Chlorophyll Functionalized Carbon Quantum Dots (Chl-CQDs) with negative charges on their surfaces are advantageous for therapeutic applications. Negatively charged surface groups can prevent proteins from binding to surfaces due to electrostatic repulsion, ensuring their prolonged circulation in the bloodstream [239][240]. However, the negative charges on CQD surfaces reduce their ability to be internalized by malignant cells [241].

Due to the structural diversity of CQDs synthesized from a variety of precursors under a variety of conditions, Chl-CQDs typically display unique qualities such as high hydrophilicity, low toxicity, and long-wavelength emission [96]. Numerous oxygen function groups, such as hydroxyl and carboxyl groups on their surface can be used to impart hydrophilicity and emission control [242]. Hydrophilicity is a critical property of biological materials that is mostly determined by the precursors used and the synthetic conditions used. CQDs have been shown to be very hydrophilic due to the hydrophilic functional groups surrounding their edges. CQDs with a high hydrophilicity have been frequently used to enhance the efficacy of tumour theranostics. According to previous research, the practical application of anticancer medicines is typically constrained by their low hydrophilicity [243]. CQDs with a high hydrophilicity can act as effective drug transporters, hence increasing therapeutic efficacy. Another significant attribute of biological materials is their low

toxicity[244]. Numerous studies have established that the majority of CQDs are generally nontoxic in vivo and in vitro. As a result of their low cytotoxicity, which is a significant characteristic of carbon dots, they have a lot of potential in the field of in vivo and in vitro biology [242]. Additionally, the carbon dots fluorescence wavelength is wavelength dependant in particular wavelength ranges, which makes them more versatile in application. Chl-CQDs created significant amounts of reactive oxygen species (ROS), which have the potential to be employed as novel nanomedicines treating malignancies[245]. The binding of chlorophyll molecules to the surface of CQDs resulted in a decrease in the energy level difference between the chlorophyll molecules, which increased ROS formation [246]. Carbon dots fluorescence properties are determined by their size, crystallinity, and functional groups.

The main objective of this study is to provide a simple, green, and low-cost hydrothermal technique for producing CQDs using chlorophyll-rich Banana leaves as a precursor. Chl-CQDs typically have unique features, such as negative charge, high hydrophilicity, low toxicity, and long-wavelength emission due to the presence of chlorophyll. In the present study we explored the free radical activity of Chl-CQDs and their cytotoxic effects on the human cancer cell lines HEK-293 and SiHa.

6.2 Results

6.2.1 Characterization of Chl-CQDs

The transmission electron microscopy (TEM) images (Figure *6.1* a) revealed that the Chl-CQDs were spherical in shape, monodisperse in size, and exhibited a restricted size distribution. The Chl-CQDs had an average diameter of 3.6 nm as shown in Figure *6.1* (a) inset.

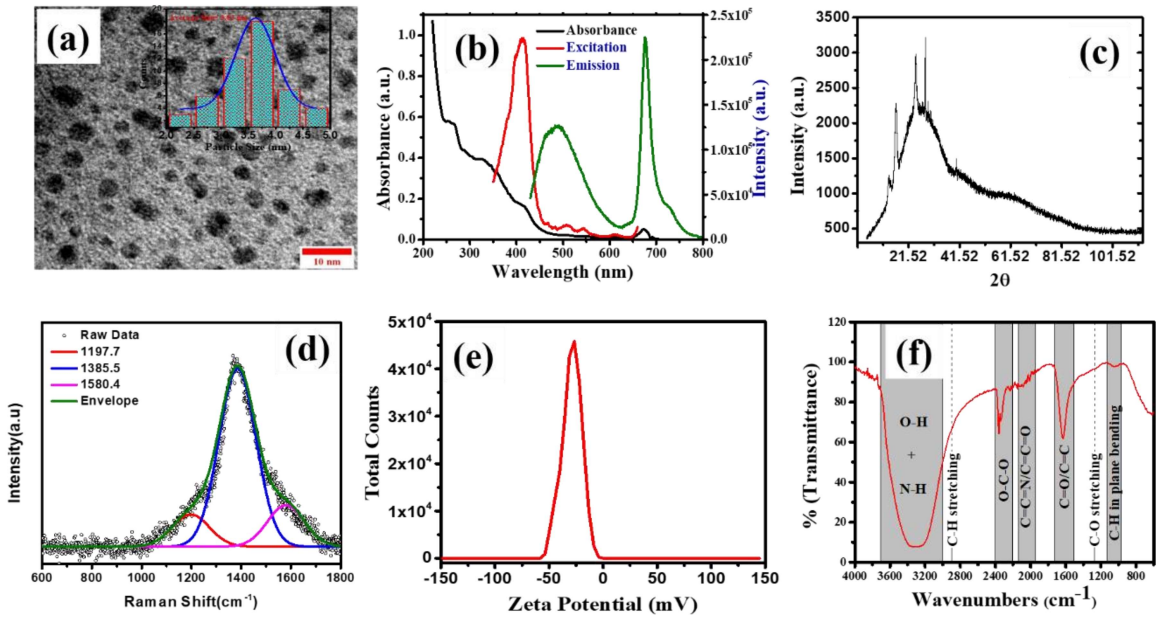

Figure 6.1 Characterization of as synthesized Chl-CQDs Concentration 1 µg/ml Chl-CQDs in DI water (a) TEM image of Chl-CQDs inset: histogram illustrating the size distribution (b) UV-Vis absorbance spectra, Excitation and Emission spectra recorded at 410 nm excitation wavelength (c) XRD pattern of Chl-CQDs (d) Raman Spectroscopy of the Chl-CQDs (e) Zeta potential (f) FTIR spectrum

The UV–Vis spectra, excitation spectrum, and emission spectrum of the Chl-CQDs are shown in Figure *6.1* (b). The optical absorptions between 230 and 320 nm, with a visible tail caused by the π - π* transition of C = C and the n- π* transition of C = O, respectively [243]. Chl-CQDs absorption properties are mostly determined by their surface functional groups or chemical composition, their size and shape of π-domains. Additionally, Chl-CQD revealed a faint peak at 414 nm and sharp peak at 675 nm, which is a chlorophyll characteristic peak [247]. Chl-CQDs having a long absorption wavelength (>650 nm) are regarded promising options for tumour diagnostics and therapeutics [243]. In comparison to higher-energy light irradiation, it has been established that red and near-infrared (NIR) light cause less photodamage and penetrate deeper into the tissue. Additionally, we demonstrated the diluted

Chl-CQDs in room light (Figure *6.2* a) and UV light (365 nm) (Figure *6.2* b). Pink fluorescence observed under extended UV radiation (365 nm) also showed the production of Chl-CQDs. The photoluminescence (PL) emission and excitation spectra of the Chl-CQDs, concentration 1µg/ml in DI water were used to evaluate their optical characteristics at room temperature. When a 410 nm excitation wavelength was used, the fluorescence spectrum of Chl-CQDs revealed a faint Chl-CQDs emission peak at approximately 500 nm and a strong chlorophyll emission peak at 675 nm [246]. Excitation-independent PL behavior is reported to be associated with fewer surface defects and a more uniform size distribution of chlorophyll-containing Chl-CQDs, which is consistent with TEM results. This result demonstrated that the prepared Chl-CQDs surfaces are chlorophyll-rich and the initial peak at 500 nm is due to different size distribution, defects and inherent photoluminescence property of Chl-CQDs [191]. At 675 nm, the full width at half maximum (FWHM) of Chl-CQD is approximately 23 nm.

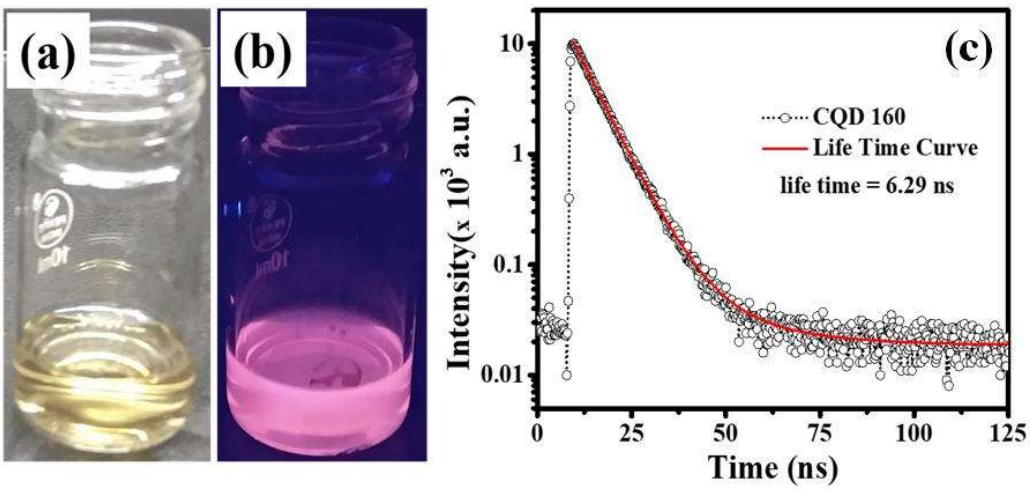

Figure 6.2 CQDs in (a) normal light and (b) exposed with UV light at wavelength 365 nm (c) Lifetime of the CQDs

Additionally, we exhibited a thin film of Chl-CQDs on a glass substrate in a Florescence microscope using a laser source with a variable wavelength (Figure *6.3*). No fluorescence was found under white light, however green fluorescence was observed between 482 and 532 nm, and pink fluorescence was observed between 586 and 646 nm. At room temperature, Chl-CQDs have a photo luminescent lifetime of 6.3 ns, as determined by a biexponential function with an R^2 value of 0.99973. (Figure *6.3* (c)).

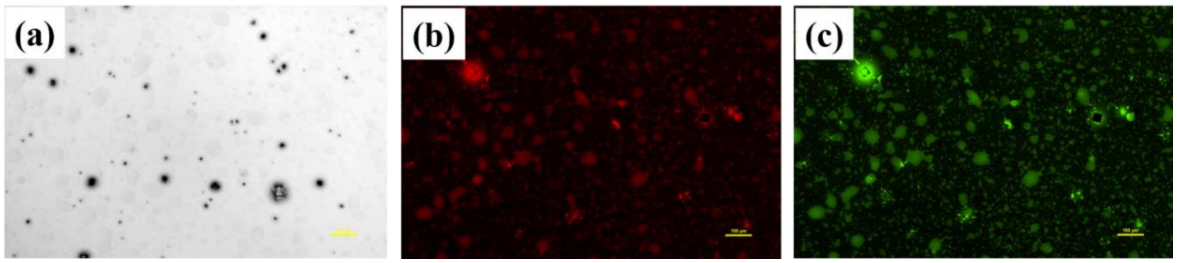

Figure 6.3 (a) Optical Characterization of CQDs (b) Fluorescence microscopic images of the CQDs at different Wavelength

Multi exponential emission decay in frequently observed in Chl-CQDs because of fast band gap transitions between different discrete energy states or because of the rapid radiative recombination of multiple exciton species that are made up of carboxyl, hydroxyl, chlorophyll and oxygen atoms [248]. The generated Chl-CQDs are well suited for cell bioimaging and exhibit a high degree of internalisation in various cells. As a result, we offer a novel method for the manufacture of highly fluorescent Chl-CQDs with tremendous promise for biological imaging and engineering [249]. The Chl-CQDs relative quantum yield (QY) was also determined by comparison to a reference fluorophore, Rhodamine 6G (which has a quantum

yield of 95% when dissolved in ethanol) [250]. QY was calculated using equation (1) at a 410 nm excitation wavelength.

$$\phi_s = \phi_r \left(\frac{I_s}{I_r}\right)\left(\frac{A_r}{A_s}\right)\left(\frac{n_s^2}{n_s^2}\right) \qquad Equation - 1$$

Where Φ, I, A, and n denote quantum yield, integrated luminescence intensity, absorbance and refractive index of the medium respectively. The abbreviations r and s denote reference (Rhodamine 6G) and sample (Chl-CQD), respectively. The Chl-CQDs relative QY was calculated to be 42 percent.

The XRD pattern shows discrete diffraction peaks at 13.78, 16.52, 24.32, 28.17, and 40.26°, showing that the carbon atoms are disordered but have a crystalline structure. A large diffraction peak centered on 26° is attributable to extremely disordered carbon atoms and 002 plane found in Chl-CQDs, confirming their amorphous nature as shown in (Figure *6.1* c) [251]. Similar to graphite, the product exhibits extremely disorganized carbon atoms. Further investigation of the unsaturated carbon bonds was conducted using the Raman spectroscopy, the Raman spectra were deconvoluted using Lorentzian peaks. We observe a large peak at 1385 cm^{-1} associated with disorder or defect related peak (D peak) and small peak at 1580 cm^{-1} corresponds to the in- plane vibrational mode of sp^2 graphitic carbon (G peak) (Figure *6.1*-d). The G-band (sp^2 hybridization) corresponds to the degree of graphitization in Chl-CQDs, whereas the D-band (sp^3 hybridization) corresponds to the amount of functionalization group and defect present. [252]. This broad convoluted D and G peaks indicates the presence of large number of defect states or surface functional groups. There is also a small peak at 1192 cm^{-1} originates from the sp^3 orbital to (D* peak) [214].

Figure *6.1*-e illustrates the zeta potential of the synthesized Chl-CQDs. According to DLS data, Chl-CQDs have a zeta potential of around -28.98 mV, a conductivity of 0.02354 mS/cm, and a Quality factor of 1.835. Negative potential indicates that the surface of Chl-CQDs contains negatively charged moieties. Chl-CQDs disperse easily in a water-based solvent due to their negative charge.

Moreover, a FTIR spectroscopy was used to determine the functional groups present on the surfaces of Chl-CQDs. The FTIR spectra of Chl-CQDs are presented in Figure *6.1*-f, along with the relative intensities of a few bands. O-H/N-H stretching vibrations are between 3410 and 3090 cm^{-1}, showing that -OH is formed in association with Chl-CQDs [253]. Additionally, the band between 1240 and 1655 cm^{-1} is attributed to the skeletal vibrations of aromatic rings. To be more precise, the absorption maxima at 1656, 1597, and 1282 cm^{-1} are consistent with C=O, C=C, and C-O stretching, respectively [254]. The existence of stretching vibration bands at 2954–2848 cm^{-1} and 900–1100 cm^{-1} demonstrates the existence of aliphatic C–H and C–C/C–N functional groups [255]. Additionally, the presence of distinctive C–H stretching and bending vibrational bands, as well as stretching vibrations for Chl-CQDs, in aromatic hydrocarbons at 3040 cm^{-1}. Around 1066 cm^{-1}, the band indicated the presence of C–O (hydroxyl, ester, epoxide, or ether) groups [253]. As a result of this confirmation, the FTIR analysis verifies the presence of several functional groups on the surface of Chl-CQDs, including alcohols, amines, aromatic rings, and carbonyls.

XPS analysis was used to assess the chemical bonding and chemical composition of the Chl-CQDs. Figure *6.4* a–d illustrates the full-scan and high-resolution XPS (HR-XPS) spectra of C1s, O1s, and N1s. Figure *6.4*-a illustrates the entire survey spectrum of Chl-CQDs, with notable peaks at 285, 400, and 532 eV corresponding to C1s, N1s, and O1s, respectively [256].

The C1s peak may be deconvoluted into six peaks at 284.2, 284.8, 285.7, 286.5, 287.6, and 288.9 eV using Lorentzian Asymmetric peak shape fit, which corresponds to aromatic C=C, C-C, C-O/C-N, C-O-C, C=O, and O-C=O groups, respectively [257][258]. Due to the presence of the ester bond, the carboxylic acid peak occurred at 288.9 eV in Chl-CQDs. Similarly, the O1s peak of Chl-CQDs can be deconvoluted into five peaks at 530.6, 531.6, 532.3, 533.0, and 533.8 eV, which correspond to the O-O, C-O, C=O, C-O-H, and O-C=O groups (Figure *6.4* c).

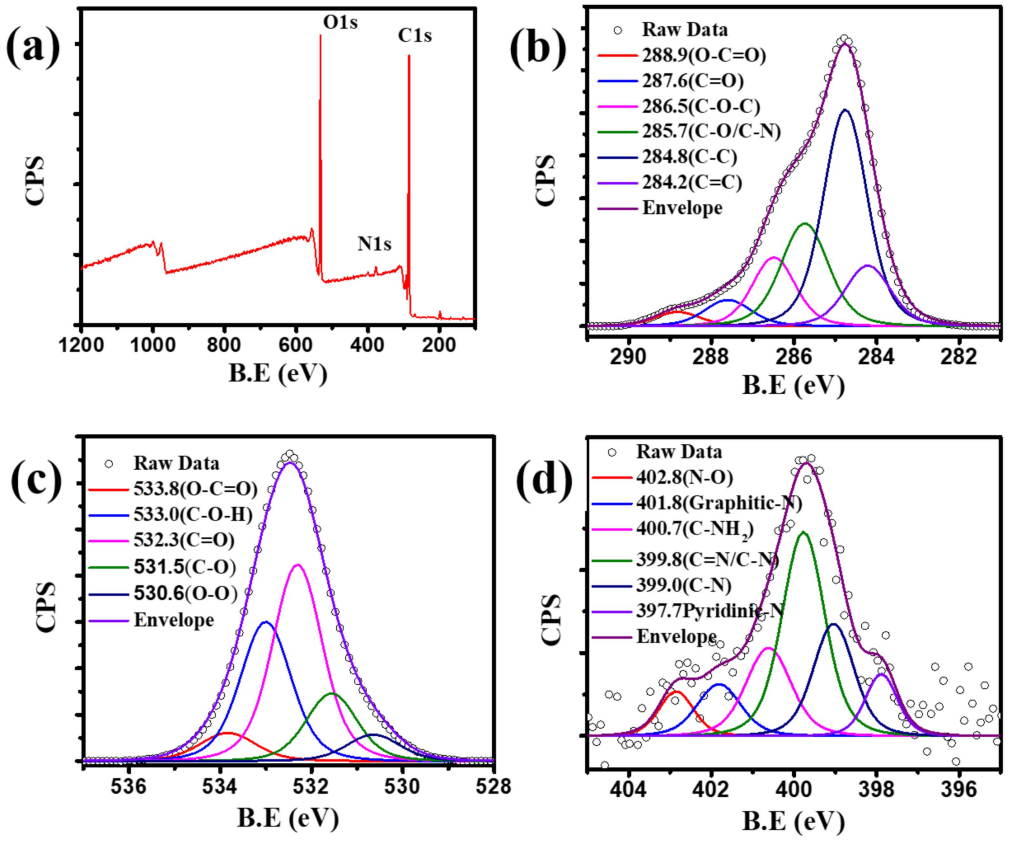

Figure 6.4 XPS Analysis of Chl-CQDs: (a) XPS Survey spectrum (b) Deconvolution of C1s (c) Deconvolution of O1s and (d) Deconvolution of N1s

Additionally, the O1s spectrum established the existence of the C-O-C bond. These functional groups get a higher solubility and stability in water. The N1s peak can be deconvoluted into six peaks at 397.9, 399.0, 399.8, 400.6, 401.8, and 402.8 eV, which correspond to Pyridinic-N, C-N, C=N, C-NH2, Graphitic-N, and N-O, respectively as shown in *Figure 6.4* (d) [259].

6.2.2 Free Radical scavenging Activity

The DPPH (2,2-Diphenyl-1-picrylhydrazyl) technique was used to measure the free radical scavenging activity of Chl-CQDs. Fresh DPPH methyl alcohol solution (100 μM) was produced in the dark. Varying quantities of Chl-CQD were diluted with DI water and volume was produced up to 1 ml to prepare primary working solutions of different concentrations [260]. Then, 1 mL of each of the preceding primary working solutions was added to 2 mL of produced DPPH solution to obtain Chl-CQDs samples ranging in concentration from 0 to 100 μg/ml in a total amount of 3 ml. The samples were then incubated for 30 minutes in a dark atmosphere. The activity of free radicals was reported as a percentage of scavenging and was estimated using Equation 2.

$$\% \text{ Scavenging} = \frac{(Ar - As)}{Ar} \times 100 \qquad \text{(Eq. 2)}$$

Where, Ar denotes the absorbance of DPPH radicals in the absence of a sample or Chl-CQDs, and As is the absorbance of DPPH radicals at 517 nm in the presence of Chl-CQDs. We measured the concentrations of samples and standards that inhibit DPPH radicals by 50% (IC50). DPPH is a free radical that contains nitrogen. When DPPH reacts with antioxidants, it takes hydrogen atoms and transforms into DPPH-H, resulting in a color change from deep violet to pale yellow [261]. We determined the amount of residual DPPH radical in the solution by comparing the absorbance intensity at 517 nm to the appropriate blank and

calculating the percent scavenging. This is confirmed visually by the colour change of the DPPH solution in the presence of Chl-CQDs from deep violet to pale yellow (Figure *6.5* a). A progressive decrease in absorbance intensity was seen as the concentration of Chl-CQDs was increased (0–100 µg/ml), suggesting its ability to scavenge free radicals (Figure *6.5* b). We discovered a polynomial association (R^2 = 0.998) between the concentrations of DPPH and Chl-CQDs in the range of 0–100 µg/ml. The dose-dependent linear scavenging activity of Chl-CQDs (from 0-30 µg/ml) was found, with the regression equation y = 1.6989x + 0 and an R^2 value of 0.998 achieved as shown in Figure *6.5* (b) inset. The IC_{50} value was found to be 29.4 µg/ml.

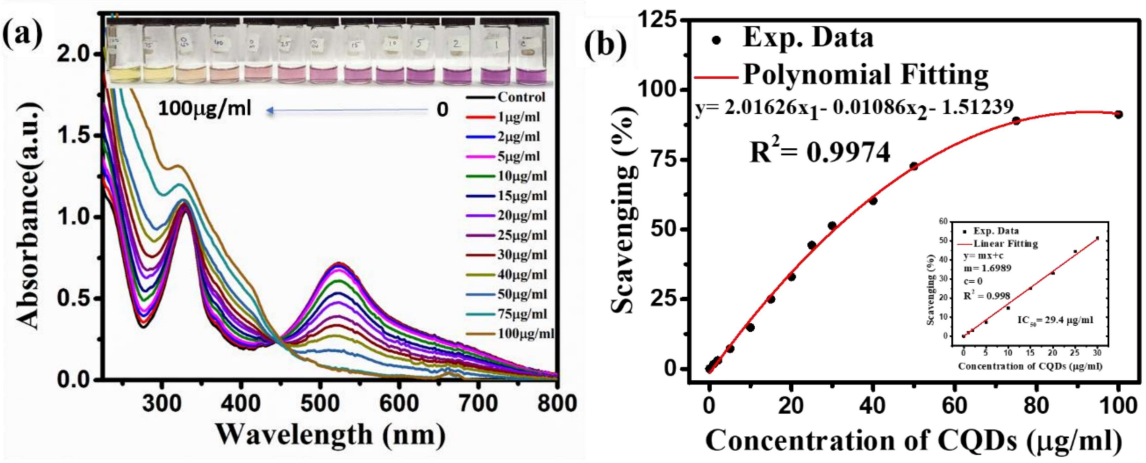

Figure 6.5 Free radical (2,2-diphenyl-1-picrylhydrazyl) activity by adding of Chl-CQDs at different Concentrations (a) Absorption spectra of DPPH upon a gradual increment of Chl-CQDs from 0 to 100 µg/ml Inset and Visual observation of DPPH Solution upon a gradual increment of Chl-CQDs from 0 to 100 µg/ml Inset: Linear Fitted Curve from 0 to 30 µg/ml.

6.2.3 Chl-CQDs suppresses the cell viability of cancer cell

Our results of MTT assay depicted that the Chl-CQDs inhibited the proliferation of cervical cancer cell SiHa but no death was noticed in normal kidney cells HEK-293 as shown in

Figure *6.6*. With increasing concentration of drug the viability of SiHa cells was found to be decreased but no cytotoxic effect on HEK-293 was reported. For instance, when SiHa cells were subjected to 100 µg/ml for 24 and and 48 hours the cell viability was found to be reduced by 50.69 % and 42.82 % respectively. The inhibitory concentration (IC50) values of Chl-CQDs in SiHa cells was calculated after 24 and 48 hours of treatment are shown in Table *6-1*.

Table 6-1 The inhibitory concentration (IC50) values of Chl-CQDs in SiHa cells was calculated after 24 and 48 hours of treatment

Compound	24 h	48 h
CQD	99.21 Mm	76.21 µM

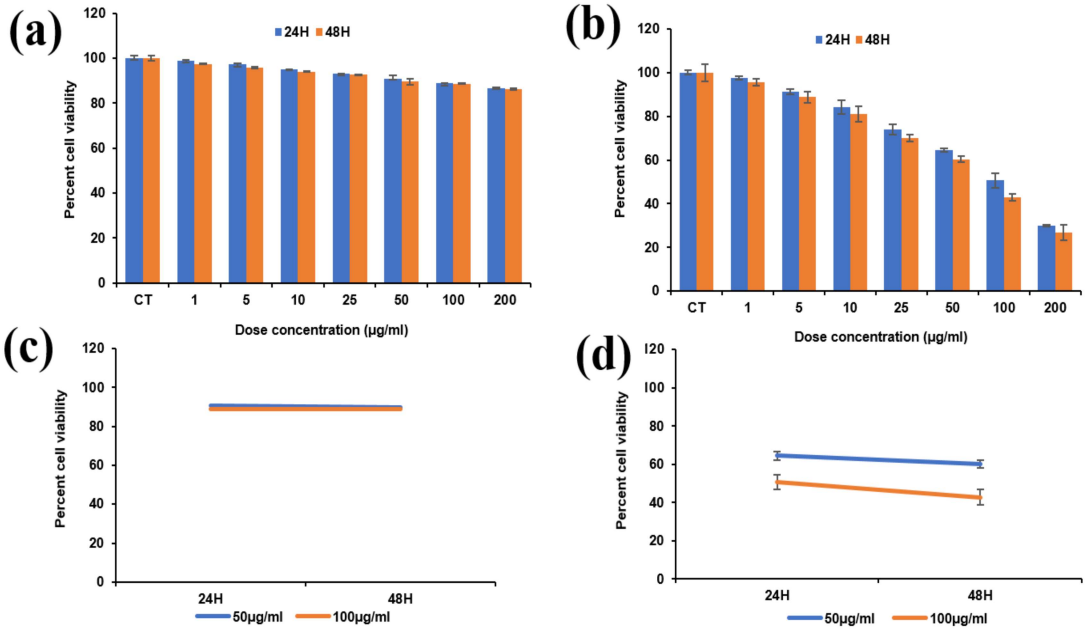

Figure 6.6 Dose dependent effect of Chl-CQDs on the proliferation of cervical cancer cell line. HEK-293 and SiHa cells were exposed to indicated concentrations of doses and the cell viability was assayed using MTT as a substrate by taking absorbance at 570 nm

6.2.4 Chl-CQDs promotes morphological changes in SiHa cells

Our phase contrast microscopic images depicted that Chl-CQDs promoted the morphological alterations including cell shrinkage, uneven form, and separation from the surface in SiHa cells but no morphological changes were observed in HEK-293 cells. For instance, at a dose of 100 µg/ml, a decrease in the number of viable cells and an increase in the number of dead cells was noticed in SiHa cells but the above-mentioned parameters were readily apparent in HEK-293 cells as shown in Figure *6.7*.

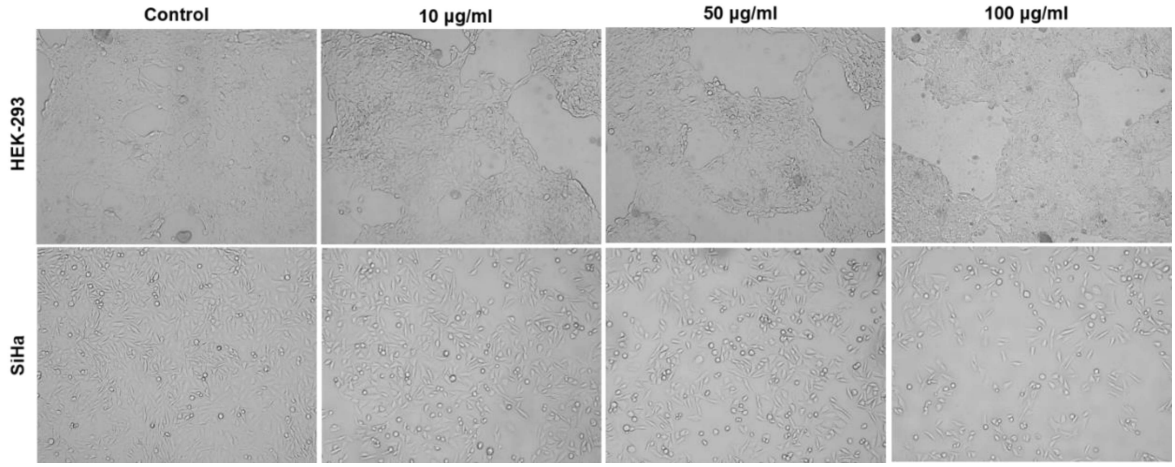

Figure 6.7 The phase contrast microscopic images of control and treated SiHa and HEK-293 cells at 10X magnification. In case of HEK-293 cells no morphological death was observed at the mentioned concentration while in case of SiHa cells Chl-CQD promoted the morphological changes including irregular shape of cells, detachment from the monolayer surface, and decreased the number of viable cells compared to control

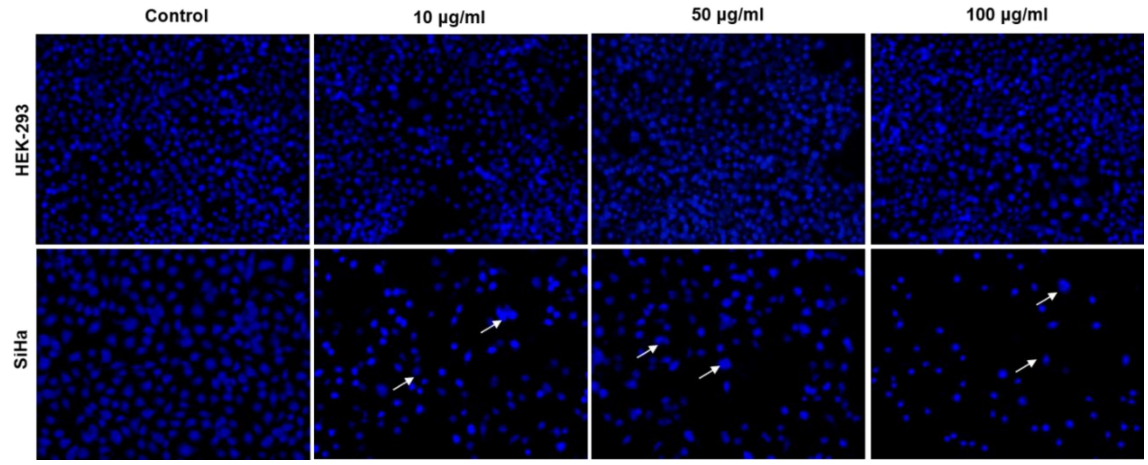

Figure 6.8 The morphological changes in the cell nucleus was observed by DAPI staining under fluorescence microscope at 20X magnification. In case of control and treated HEK-293 cells round and oval shaped nuclei was observed while in case of treated SiHa cells nuclear fragmentation with nuclear apoptotic bodies was observed

6.2.5 Chl-CQDs promotes nuclear changes in SiHa cells

Our results of DAPI staining indicated that in case of HEK-293 cells the nuclei were oval or spherical shaped while in case of SiHa cells nuclear apoptotic bodies and fragmented cell nuclei were observed as shown in Figure *6.8* . For example, after 24 hours of exposure to Chl-CQDs at a concentration of 100 µg/mL, fragmented nuclei were observed in SiHa cells. For instance, when cells were exposed to metal complex for 24 h at a concentration of 100 µg/ml, the fragmented cell nuclei was observed.

6.2.6 Chl-CQDs promotes apoptosis in SiHa cells

Our results of AOPI staining revealed that in case of HEK-293 cells, only viable cells emitted the green fluorescence and no red fluorescence was noticed whereas in SiHa cells viable cells emit green fluorescence while dead cells emitted red fluorescence which indicates the

decrease in the number of viable cells and increase in the number of apoptotic cells as shown in Figure *6.9*.

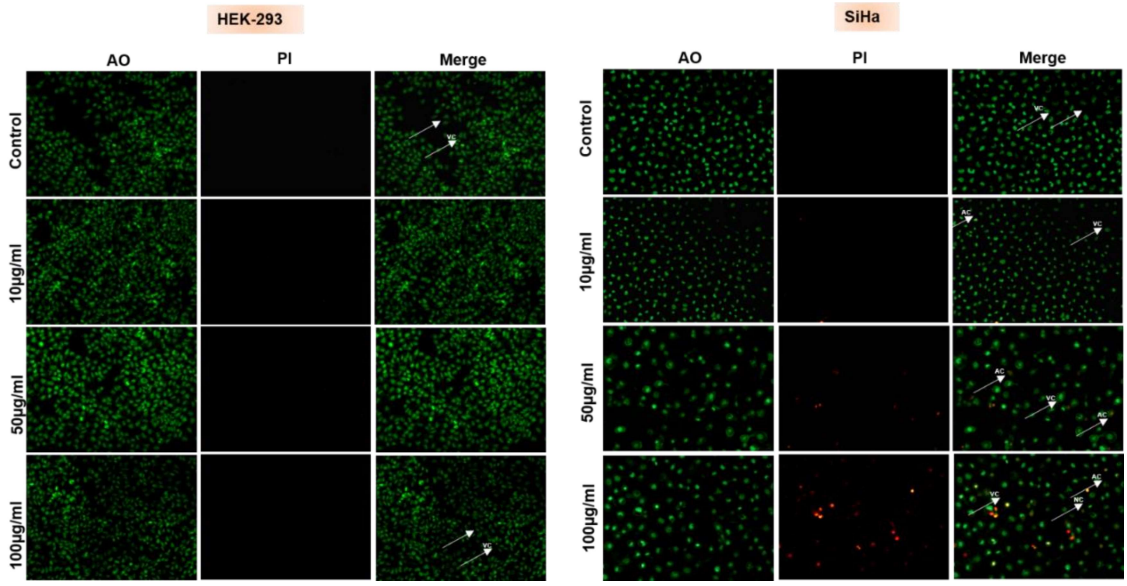

Figure 6.9 Fluorescence microscopy images of HEK-293 and SiHa cells stained with AO/PI after treatment with indicated concentration of Chl-CQDs for 24 hours. Control cells exhibit uniformly stained intact green nucleus representing viable cells while in treated cells appearance of bright orange to uniform orange coloured nucleus were observed representing apoptotic and necrotic cells respectively

For example, after 24 hours of exposure to Chl-CQDs at a concentration of 100 µg/mL, no apoptotic and necrotic cells were observed in HEK-293 cells while in case of SiHa cells a decrease in the number of viable cells (green fluorescence) and an increase in the number of early apoptotic (red fluorescence) and late apoptotic (orange fluorescence) cells were observed.

6.2.7 Chl-CQDs promotes plasma membrane damage in SiHa cells

The effect of Chl-CQDs on plasma membrane integrity was evaluated by measuring LDH leakage into the culture medium and our results showed that after treating the cells with

various concentrations of Chl-CQDs the integrity of plasma membrane is maintained and no damage was reported. However, in SiHa cells the Chl-CQDs treatment damaged the plasma membrane and released the LDH in the culture medium. For instance, at a concentration of 100 µg/mL of Chl-CQDs, no damage to the cells was observed in HEK-293 cells because of no rise in LDH activity while in case of SiHa cells 2.65 fold increase in the LDH activity was observed that reflects the damage to the cell membrane as shown in Figure *6.10*.

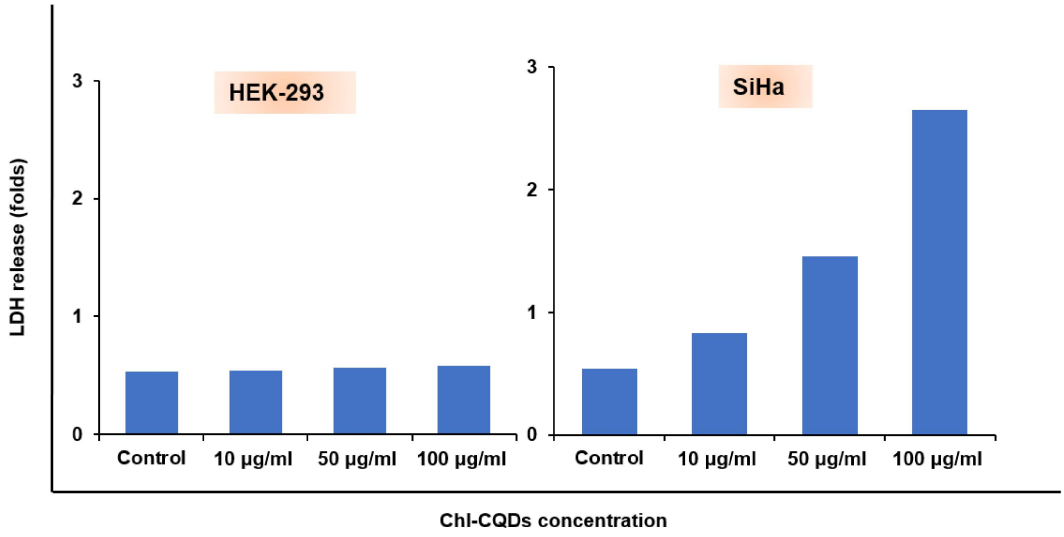

Figure 6.10 . The released LDH content into the culture medium was measured after 24 hours to reflect the cell death in response to Chl-CQDs treatment. In case of HEK-293 cells no cell death was reported because of no rise in LDH activity while concentration-dependent rise in the LDH activity reflects the cell death in case of SiHa cells

6.3 Discussion

Cervical cancer is the most frequently diagnosed female reproductive disease in the world. Cervical cancer occurs at a higher rate in developing countries than in industrialized countries. Despite the fact that the majority of anticancer medications are used to treat cervical cancer, their overall efficacy remains limited [262]**.** Recent advances in nanotechnology have led in

significant advancements in the use of quantum dots not only for the development of new anticancer drugs, but also for the treatment of a variety of cancers [195]. Now a days the recruitment of Chl-CQDs makes them an excellent agents for biological applications because of its unique optical properties including outstanding solubility in water, great sensitivity and selectivity for target analytes, disease detection capabilities, low toxicity, favorable biocompatibility, and excellent photo stability [263]**.** Despite these optical properties Chl-CQDs also possesses some excellent electrical properties including quantum confinement effect, which is dependent on the size and composition of the nanoparticles [264]. CQDs are semiconductor nanocrystals with smaller than the Bohr excitation radius in terms of physical dimensions, most notably the renowned display for Chl-CQDs with changing semiconductor nanoparticle sizes [265]. All these attributes of Chl-CQDs ignited the curiosity of biomedical professionals, who are now studying a wide variety of potential bio-applications that are already demonstrating viability. As a result of this effort, Chl-CQDs were synthesized using banana leaves as a source and investigated for its anticancer efficacy using FTIR, XPS, UV-Vis, TEM, Raman and fluorescence spectroscopy. The average size of Chl-CQDs was determined to be 3.6 nm, and they were functionalized with alcohols, amines, aromatic rings, carbonyls, and chlorophyll. Which is very hydrophilic in nature and is easily soluble in DI water.

For the first time, we investigated the cytotoxic potential of Chl-CQDs against normal cells (HEK-293) and cervical cancer cells (SiHa). Our findings indicated that Chl-CQDs were non-toxic and biocompatible with HEK-293 cells while imposed significant anti-cancer effect on SiHa cells hence, inhibited the proliferation of SiHa cells in a dose and time dependent manner. These observations could be explained by the following factors: (a) increased cellular

uptake due to the smaller size of Chl-CQDs, their more stable and hydrophilic suspension, and their ability to penetrate deeper into cancerous cells; (b) increased cellular uptake due to the long wavelength of chlorophyll-functionalized Chl-CQDs; (c) Chl-CQDs generated high levels of reactive oxygen species in cancer cells; and (d) Chl-CQDs with negative surface charges are preferable for therapeutic applications. Consistent with the cell viability data, the phase contrast images for both cell lines support the MTT experiment results.

Apoptosis is a highly complex process that involves a variety of morphological changes in the cells, including cell shrinkage, loss of plasma membrane integrity, chromatin condensation, and the formation of apoptotic bodies [266]**.** In recent years, CQDs have been investigated for their capacity to penetrate cancer cells. CQDs with a high QY, stability, and long-wavelength emission, particularly in the near infrared, are essential for the development of fluorescence imaging probes. As a proof of concept, the Chl-CQD was dissolved in medium and utilised to image and treat self-targeted cancer cells. Our fluorescence imaging results indicated that Chl-CQDs had no cytotoxic effect on HEK-293 cells but promoted apoptosis in SiHa cells, as indicated by cell shrinkage, loss of plasma membrane integrity, membrane blebbing, nuclear fragmentation, decreased viable cells, and increased apoptotic cells. In summary, the findings of this study reveal that Chl-CQDs are biocompatible with HEK-293 cells but oncostatic with SiHa cells.

6.4 Conclusion

In summary, we produced a novel carbon nanomaterial with Chl-CQDs for the first time. This method of production has several advantages, including ease of preparation, low cost of raw material (banana leaf), and environmental friendliness. The Chl-CQDs generated exhibit desirable properties such as high fluorescence intensity, excellent water solubility, and

biocompatibility. The cumulative results defines that the Chl-CQDs possess enormous therapeutic potential against cervical cancer without imposing any cytotoxic effect in normal cells. Hence, the Chl-CQDs might be executed as a new fluorescent medicine not only against cervical cancer but also against other chronic diseases without insulting the human's life. In addition, further *in vivo* and clinical trials are necessary for the evaluation of its anticancer attribute to accomplish above mentioned statement before implementing for the benefit of society.